Decreased Craniocervical CSF Flow in Patients with Normal Pressure Hydrocephalus: A Pilot Study

S.M. Stöcklein, M. Brandlhuber, S.S. Lause, A. Pomschar, K. Jahn, R. Schniepp, N. Alperin, and B. Ertl-Wagner

ABSTRACT

BACKGROUND AND PURPOSE: Normal pressure hydrocephalus is characterized by systolic peaks of raised intracranial pressure, possibly due to a reduced compliance of the spinal CSF spaces. This concept of a reduced spinal CSF buffer function may be reflected by a low cervical CSF outflow from the cranium. The aim of this study was to investigate craniospinal CSF flow rates by phase-contrast MR imaging in patients with normal pressure hydrocephalus.

MATERIALS AND METHODS: A total of 42 participants were included in this prospective study, consisting of 3 study groups: 1) 10 patients with normal pressure hydrocephalus (mean age, 74 [SD, 6] years, with proved normal pressure hydrocephalus according to current scientific criteria); 2) eighteen age-matched healthy controls (mean age, 71 [SD, 5] years); and 3) fourteen young healthy controls (mean age, 21 [SD, 2] years, for investigation of age-related effects). Axial phase-contrast MR imaging was performed, and the maximal systolic CSF and total arterial blood flow rates were measured at the level of the upper second cervical vertebra and compared among all study groups (2-sample unpaired *t* test).

RESULTS: The maximal systolic CSF flow rate was significantly decreased in patients with normal pressure hydrocephalus compared with age-matched and young healthy controls (53 [SD, 40] mL/m; 329 [SD, 175] mL/m; 472 [SD, 194] mL/m; each $P < .01$), whereas there were no significant differences with regard to maximal systolic arterial blood flow (1160 [SD, 404] mL/m; 1470 [SD, 381] mL/m; 1400 [SD, 254] mL/m; each $P > .05$).

CONCLUSIONS: The reduced maximal systolic craniospinal CSF flow rate in patients with normal pressure hydrocephalus may be reflective of a reduced compliance of the spinal CSF spaces and an ineffective spinal CSF buffer function. Systolic craniospinal CSF flow rates are an easily obtainable MR imaging–based measure that may support the diagnosis of normal pressure hydrocephalus.

ABBREVIATIONS: ACB_{max} = maximal arterial blood flow rate to the brain during systole; CSF_{max} = maximal CSF flow rate from the brain to the spinal canal during systole; DESH = disproportionately enlarged subarachnoid space hydrocephalus; HC-M = age-matched healthy controls; HC-Y = healthy young controls; Ø = diameter; NPH = normal pressure hydrocephalus; VENC = velocity-encoding

Normal pressure hydrocephalus (NPH) is the most frequent form of hydrocephalus in elderly patients.[1] It is characterized by the clinical syndrome of progressive gait disturbance, cognitive deficits, and urinary incontinence, the so-called Hakim-Adams triad.[1] NPH has been shown to be responsive to CSF shunting, with the likelihood of symptom improvement better in the early stages of the disorder,[2,3] emphasizing the importance of an early diagnosis. However, the diagnosis of NPH remains a major challenge.

Typical imaging findings in NPH include ventricular enlargement with an Evans index of >0.31,[4] a narrow callosal angle (< 90°),[5] periventricular high-signal changes representing transependymal cerebral fluid egress,[6,7] tight sulci in the convexities of the cerebral hemispheres,[8] and an enlarged Sylvian fissure (disproportionately enlarged subarachnoid space hydrocephalus [DESH] criteria).[4]

Phase-contrast MR imaging allows the quantification and characterization of pulsatile flow with high spatial and temporal resolution.[9] Arterial inflow, venous outflow, and CSF flow to and from the brain can be quantified in relation to the cardiac cycle.[9] Several studies have described higher CSF oscillations at the level

Received May 31, 2021; accepted after revision October 16.

From the Departments of Radiology (S.M.S., M.B.), Neurology, and Friedrich-Baur-Institute (FBI) of the Department of Neurology (K.J.), and Neurology (R.S.), Ludwig-Maximilians-University Munich, Munich, Germany; Department of Dermatology (S.S.L.), Bethesda Hospital, Freudenberg, Germany; Radiological Office (A.P.), Centre for Radiology, Munich, Germany; Department of Radiology (N.A.), University of Miami, Coral Gables, Florida; and Department of Medical Imaging (B.E.-W.), The Hospital for Sick Children, University of Toronto, Toronto, Ontario, Canada.

S.M. Stöcklein and M. Brandlhuber contributed equally to the study.

Please address correspondence to Martina Brandlhuber, MD, Department of Radiology, Ludwig-Maximilians-University Munich, Marchioninistr 15, 81377 Munich, Germany; e-mail: Martina.Brandlhuber@med.uni-muenchen.de

http://dx.doi.org/10.3174/ajnr.A7385

Table 1: Participant demographics

	NPH	HC-M	HC-Y
Study participants (No.)	10	18	14
Sex (female/male)	8/2	11/7	8/6
Age (mean) (min/max) (yr)	74 (SD, 6.2) (60/82)	71 (SD, 5.3) (60/86)	21 (SD, 1.7) (19/24)

Note:—Max indicates maximum; min, minimum.

of the aqueduct[10-12] as well as lower total cerebral blood flow at the cervical level in patients with NPH.[11,13,14]

The pathophysiology of NPH has not been fully elucidated. Chronic hypertension may cause periventricular ischemia,[15,16] resulting in ventricular enlargement[15,16] and reduced compliance of the CSF spaces.[17] Periventricular ischemia may also locally increase venous resistance, leading to a decrease of CSF absorption, thereby further contributing to ventricular enlargement.[18] New concepts have attributed the pathophysiology of NPH to abnormal dynamics of CSF and blood flow,[19-23] including hyperdynamic CSF flow in the aqueduct, reduced cerebral blood flow,[22] increased CSF pulse pressure, and pathologic conditions of CSF reabsorption.[18] Despite the name, intracranial pressure is not always normal in NPH;[24] systolic peaks of raised intracranial pressure are frequently observed.[20] In healthy individuals, CSF outflow compensates for systolic intracranial volume peaks to avoid increased pressure.[24] In patients with NPH, the systolic intracranial pressure peaks may be due to a reduced compliance of the spinal CSF spaces, which may be reflected by an inefficient craniospinal CSF outflow. To our knowledge, craniospinal CSF flow in the upper cervical spine has not been assessed in patients with NPH.

We, therefore, aimed to investigate spinal craniospinal CSF flow rates in patients with NPH and compare them with those in age-matched and younger healthy controls. We hypothesized that craniospinal CSF outflow is reduced in patients with NPH as a sign of a lowered buffer function of the spinal CSF spaces. Moreover, we intended to provide an MR imaging–based tool that may help diagnose NPH using instrumental instead of clinical metrics.

MATERIALS AND METHODS

Subjects

Institutional review board (Ethics Committee of the Medical Department, LMU Munich) approval was obtained before the study, and all subjects provided written informed consent. A total of 42 study participants were included in this prospective study (for patient demographics see Table 1). We defined 3 study groups: 1) ten patients with proved NPH according to current scientific criteria (see more details below);[25,26] 2) eighteen age-matched, healthy controls (HC-M); and 3) fourteen young healthy controls (HC-Y) for the investigation of age-related effects.

A detailed history of all participants was obtained with a special focus on neurologic and cardiovascular disorders. Exclusion criteria for all groups were MR imaging–based contraindications such as cardiac pacemakers, cochlear implants or other ferromagnetic implants; claustrophobia; and any severe non-neurologic disorder. Inclusion criteria were defined as group-specific for the NPH, HC-M, and HC-Y groups.

Before inclusion in the NPH group of the study, patients were diagnosed with NPH at the Department of Neurology at Ludwig-Maximilians-University of Munich. Diagnosis was based on clinical neurologic parameters, imaging parameters, and the lumbar tap test.

Neurologic parameters were evaluated by detailed neurologic examinations and tests. To evaluate the symptom complex of dementia, we performed several neurocognitive tests, including the Mini-Mental State Examination, psychomotor velocity during visual tracking, object recognition and naming, Verbal Learning and Recall Performance, Number Connection Test, and general linguistic competence. For assessment of gait instability, a 3D gait analysis was performed; gait pattern was analyzed by functional gait assessment, and both the Timed Up and Go test and the 10 Meter Walk Test were conducted. The symptom of urinary incontinence was identified by clinical anamnesis.

NPH was considered proved when a typical hypokinetic apractic gait disturbance was present, together with at least 1 more of the Hakim triad symptoms (dementia and/or urinary incontinence), along with no other reason for hydrocephalus and gait disturbance.

For evaluation of NPH imaging parameters, an initial CT of the brain was acquired and imaging features of NPH were assessed. NPH was considered proved if the following conditions were present: hydrocephalus with an Evans index of >0.3, tight sulci in the convexities of the cerebral hemispheres, and an enlarged Sylvian fissure (DESH criteria[4]).

The lumbar tap test (removing 30 mL of CSF through a lumbar puncture) was performed before and after neurologic testing.

To verify NPH, positive findings on a lumbar tap test were necessary, ie, an objective improvement of gait instability after the lumbar tap test. This was defined as at least 20% improvement compared with the initial performance during gait analysis, in detail, $\geq$ 20% increase of maximum walking speed measured for >10 m (10 Meter Walk Test). An objective improvement of dementia after the lumbar tap test was defined as at least 10% performance enhancement compared with the initial value during neuropsychological testing.

The inclusion criteria for the NPH group were a proved NPH diagnosed earlier at the Department of Neurology at Ludwig-Maximilians-University of Munich, a minimum of 60 years of age, and an insidious onset of symptoms with progression of symptoms during at least 3 months. The exclusion criterion for the NPH group was a secondary hydrocephalus (eg, after craniocerebral trauma or meningitis), whereas the presence of other neurologic diseases without potential influence on the development of hydrocephalus did not constitute an exclusion criterion (eg, tremor or dizziness; Table 2). For characteristics of patients with NPH, see Table 3.

The inclusion criterion for the HC-M group was a mean age (71 [SD, 5 years]) comparable with that of the patients in the NPH group (74 [SD, 6 years]). Exclusion criteria for the HC-M group were the simultaneous occurrence of at least 2 of the 3 symptoms of the Hakim triad and/or the presence of hydrocephalus. Other

exclusion criteria were diseases known to cause hydrocephalus (Table 2).

Inclusion criterion for the HC-Y group was 18–25 years of age; exclusion criteria were analogous to those of the HC-M group (Table 2).

MR Imaging and MR Imaging Flow Rates

Participants were imaged in the supine position, with legs slightly elevated to improve comfort, on a 3T MR imaging scanner (Magnetom Verio; Siemens). A phased-array head and neck coil with a total of 12 channels was used. A pulse oximeter was fixed onto the forefinger to synchronize the measurements with the cardiac cycle (R wave–triggered). MR imaging included both structural and flow MR imaging sequences.

Structural MR images consisted of an axial FLAIR sequence (TR = 7000 ms, TE = 94 ms, FOV = 250 × 175 mm^2, voxel size = 0.9 × 0.9 × 3.0 mm^3) and a sagittal 3D MPRAGE sequence (TR = 11 ms, TE = 4.76 ms, FOV = 210 × 210 mm^2, voxel size = 1.0 × 1.0 × 0.7 mm^3, integrated parallel acquisition techniques with acceleration factor = 2).

Flow imaging to measure hemo- and hydrodynamic parameters consisted of 2 retrospectively gated, velocity-encoded (VENC), cine phase-contrast sequences. To locate the correct positioning, we used a sagittal phase-contrast 2D localizer with the following parameters: TR = 19.2 ms, TE = 5.1 ms, FOV = 200 × 200 mm^2, voxel size = 1.0 × 0.8 × 35 mm^3. First, a high VENC (80 cm/s) axial sequence was acquired to quantify high-velocity blood flow in the internal carotid arteries and vertebral arteries. A second sequence with a low VENC (8–10 cm/s) was performed to quantify CSF flow. As suggested by Tain et al,[27] measurements were obtained at the level of C2, with an orientation perpendicular to the main 4 arteries (left and right internal carotid and vertebral arteries) for the high-VENC sequence and perpendicular to the spinal canal for the low-VENC sequence. Sequence parameters were as follows: TR = 40.25 ms, TE = 7.19 ms, FOV = 130 × 110 mm^2, voxel size = 0.8 × 0.5 × 6.0 mm^3. Phase-contrast imaging was performed for 32 heart cycles and took about 3 minutes, with discrete differences due to the individual heart rates of the study participants.

Table 2: Comorbidities of participants[a]

Study Group	NPH	HC-M	HC-Y
Arterial hypertension	5/10	6/18	0/14
Arteriovenous malformation	0/10	0/18	2/14
Atrial fibrillation	0/10	2/18	0/14
Headaches	0/10	1/18	1/14
Coronary heart disease	2/10	0/18	0/14
Dizziness	1/10	0/18	0/14
Meningioma[b]	0/10	1/18	0/14
Microangiopathy	1/10	1/18	0/14
Multiple sclerosis	0/10	0/18	4/14
Orthostatic tremor	1/10	0/18	0/14
Peripheral arterial disease	1/10	0/18	0/14
Restless leg syndrome	0/10	1/18	0/14
Seizure disorder	1/10	0/18	1/14
Prior stroke	1/10	3/18	0/14
History of syncope	0/10	1/18	0/14
History of transient ischemic attack	0/10	2/18	0/14

[a] Data are number of patients per study group.
[b] The meningioma measured 1.2 cm at the maximum.

Table 3: Characteristics of patients with NPH

	Characteristics	No. of Patients
Neurologic parameters (Hakim-Adams triad)	Gait disturbance	10/10
	Urinary incontinence	8/10
	Dementia[a]	8/10
Imaging parameters	Evans index >0.3	10/10
	DESH criteria	10/10
	Ventricular enlargement	6/10
	Signs of transependymal CSF diapedesis	6/10
Lumbar tap test[b]	Objective improvement of gait disturbance	10/10
	Objective improvement of cognitive function	7/10

[a] Sixty percent progressive disease (predominant impairment of short-term memory).
[b] Forty percent additionally received a tap test via a Yuohy needle lasting several days.

Postprocessing and Data Analysis

Details of the MR imaging–based measurements of arterial inflow and CSF flow to and from the brain have been described previously.[28] In brief, time-dependent volumetric flow rates were calculated by integrating the flow velocities within the luminal cross-sectional areas over all 32 phase-contrast images representing 1 cardiac cycle. This calculation was performed using the semiautomated pulsatility-based lumen-segmentation method to decrease variability.[29] Absolute flow rates were obtained for the 4 main cervical arteries (left and right internal carotid arteries; left and right vertebral arteries).

The following volumetric flow rates were defined and calculated for all participants: 1) the maximal CSF flow rate from the brain to the spinal canal during systole (CSF_{max}); and 2) the maximal arterial blood flow rate to the brain during systole (ACB_{max}). Figure 1*A*, *-B* provides an example of blood and CSF flow VENC images. All analyses were performed with MRICP software, Version 1.4.35 (Alperin Noninvasive Diagnostics).

To determine the relationship between arterial blood inflow (ACB_{max}) and CSF outflow (CSF_{max}), we calculated the ratio between both parameters for all study groups (CSF_{max}/ACB_{max}).

In addition, the minimal diameter (Ø) of the spinal canal was measured in a midsagittal MPRAGE image at the level of the intervertebral space between the second and third upper cervical vertebrae ($Ø_{C2/C3}$), (Fig 1*C*). To define the impact of spinal width on the maximal CSF outflow during systole (CSF_{max}), we performed correlation analysis between both parameters (CSF_{max} and $Ø_{C2/C3}$).

Statistical Analysis

Statistical analyses were performed using SPSS 17.0 for Windows (IBM) and Matlab (MathWorks). The independence of variables was validated by the χ^2 test. Group differences were analyzed using the 2-sample unpaired *t* test. Correlation analysis was performed using the Pearson correlation

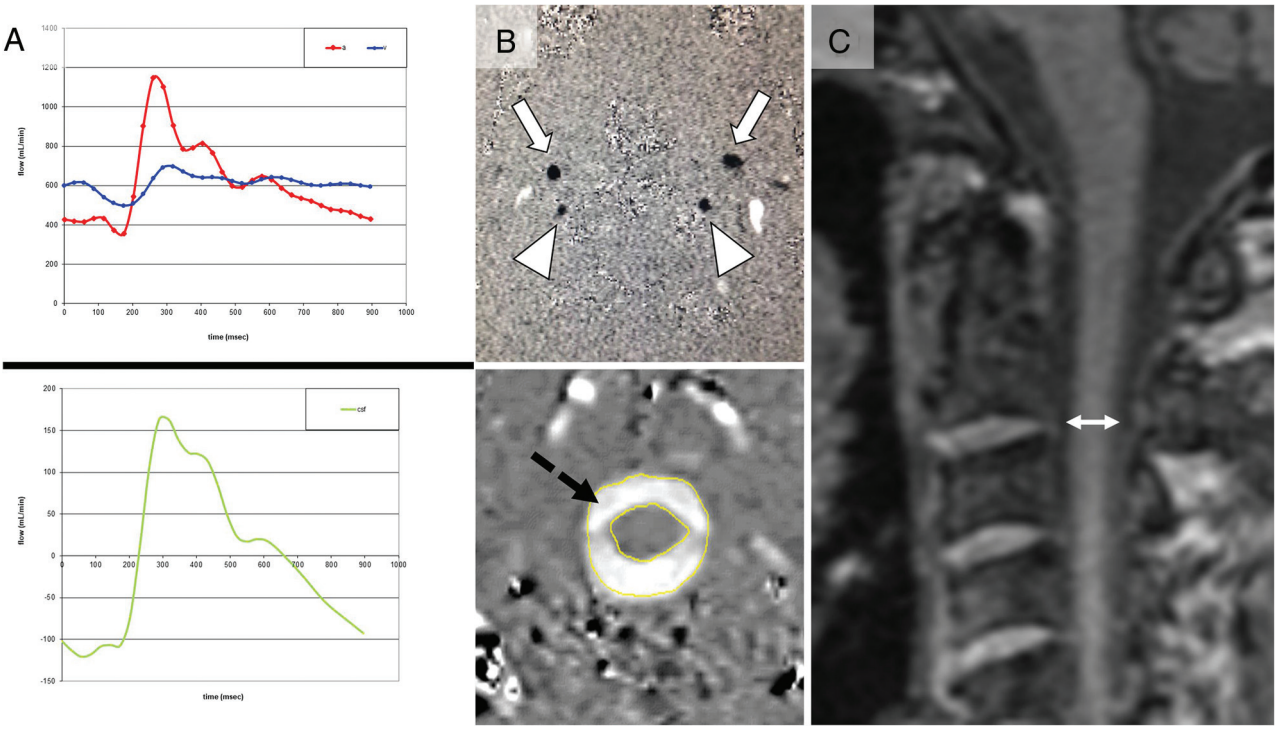

FIG 1. Measurement of CSF/blood flow and spinal canal width. *A*, Craniospinal blood and CSF flow (milliliter/minute) during the cardiac cycle across time (millisecond). The *upper panel* shows the blood flow. During each systole, arterial blood (red) flows into the cranium and venous blood flows in a cardiac direction; outflow is too slow to compensate the resulting increase in intracranial pressure. The *lower panel* shows the resulting fast CSF outflow (green) from the brain to the spinal CSF spaces to buffer pressure peaks. *B*, VENC phase-contrast MR images of blood and CSF. The *upper panel* demonstrates the blood flow through the internal carotid arteries (*arrows*) and vertebral arteries (*arrowheads*), and the internal jugular veins are represented by the *oval white spots* (not marked). The *lower panel* shows the flow of CSF (*black dashed arrow*) from the cranium to the spinal canal. Upward flow is black, while downward flow is white. *C*, Measurement (*double-sided arrow*) of the maximal diameter of the spinal canal in a midsagittal MPRAGE image at the level of the intervertebral space between the second and third upper cervical vertebrae ($Ø_{C2/C3}$) is shown.

coefficient. Data are presented as mean (SD). $P < .05$ was considered statistically significant.

RESULTS

Baseline Characteristics

Forty-two participants were included (27 women/15 men). The NPH group consisted of 10 participants (8 women/2 men); the HC-M group, 18 participants (11 women/7 men); and the HC-Y group, 14 participants (8 women/6 men). There was no significant difference between the ages of men compared with female participants for all groups, and there was no significant difference in age between the NPH and HC-M groups. For patient demographics, see Table 1; the comorbidities of the study participants are shown in Table 2. For characteristics of patients with NPH, see Table 3.

CSF_{max} from the Brain

The CSF_{max} was significantly different among the 3 study groups. Compared with the HC-M group, the mean CSF_{max} was significantly decreased in patients with NPH (NPH, 53 [SD, 40] mL/m, versus HC-M, 329 [SD, 175] mL/m; $P < .01$). Moreover, mean CSF_{max} was significantly diminished in the HC-M group compared with the HC-Y group (472 [SD, 194] mL/m, versus HC-M, 329 [SD,175] mL/m; $P < .05$; Fig 2*A*).

ACB_{max}

The mean ACB_{max} was not significantly different among the 3 study groups. ACB_{max} was 1160 (SD, 404) mL/m for patients with NPH, 1470 (SD, 381) mL/m for the HC-M group, and 1400 (SD, 254) mL/m for the HC-Y group (each, $P > .05$; Fig 2*B*).

CSF_{max}/ACB_{max}

To account for a potential impact of ACB_{max} on CSF_{max}, we calculated the ratio between both parameters for all study groups (CSF_{max}/ACB_{max}). CSF_{max}/ACB_{max} was different among the 3 study groups. The CSF_{max}/ACB_{max} was significantly decreased in patients with NPH compared with the age-matched healthy controls (mean NPH, 0.1 [SD, 0.1], versus HC-M, 0.2 [SD, 0.1]; $P < .05$). Moreover, the CSF_{max}/ACB_{max} was significantly diminished in the HC-M group compared with the HC-Y group: 0.3 (SD, 0.1), versus HC-M, 0.2 (SD, 0.1); $P < .05$; Fig 2*C*).

Minimal Diameter of the Spinal Canal

The minimal midsagittal diameter of the spinal canal ($Ø_{C2/C3}$) was different among the 3 study groups. Compared with HC-M, the $Ø_{C2/C3}$ was significantly decreased in patients with NPH (NPH, 1.25 [SD, 0.16] cm, versus HC-M, 1.36 [SD, 0.12] cm; $P < .05$). The minimal diameter of the spinal canal ($Ø_{C2/C3}$) was significantly larger in HC-Y compared with both HC-M and patients with NPH (HC-Y, 1.48 [SD, 0.08] cm, versus HC-M,

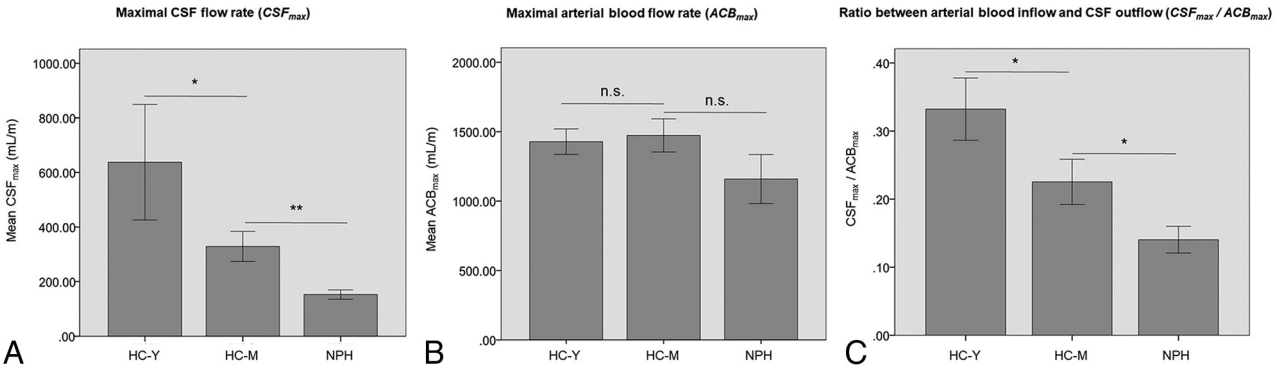

FIG 2. CSF_{max}, ACB_{max}, and the ratio between both parameters (CSF_{max}/ACB_{max}). *A*, Maximal CSF flow rate (CSF_{max}) in milliliter/minute. *B*, ACB_{max} in milliliter/minute. *C*, Ratio between arterial blood inflow and CSF outflow (CSF_{max}/ACB_{max}). The *asterisk* indicates $P < .05$; *double asterisks*, $P < .01$; n.s., not significant.

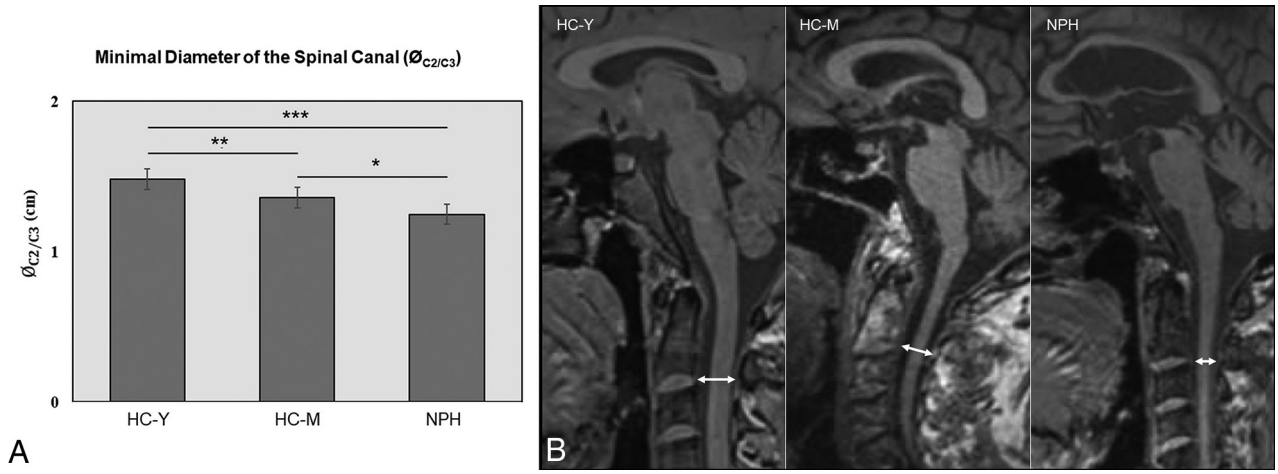

FIG 3. Minimal diameter of the spinal canal ($Ø_{C2/C3}$). *A*, Minimal diameter of the spinal canal ($Ø_{C2/C3}$) in centimeters. *B*, Representative MR images (midsagittal T1-weighted image) to measure the minimal diameter of the spinal canal at the level of the intervertebral space between the second and third upper cervical vertebrae (*double-sided arrow*). The *left panel* shows an image of an HC-Y, the *middle panel* shows an HC-M, and the *right panel* shows an image of a patient with NPH. The *asterisk* indicates $P < .05$; *double asterisks*, $P < .01$; *triple asterisks*, $P < .001$.

1.36 [SD, 0.12] cm; $P < .01$; HC-Y, 1.48 [SD, 0.08] cm, versus NPH, 1.25 [SD, 0.16] cm; $P < .001$) (Fig 3).

Correlation between Spinal Canal Diameter and Maximal CSF Outflow

To define the impact of spinal width on CSF_{max}, we performed a correlation analysis between CSF_{max} and $Ø_{C2/C3}$, and a significantly positive correlation between CSF_{max} and $Ø_{C2/C3}$ was found, showing a lower CSF_{max} with lower spinal diameter ($R = 0.47$; $P < .05$; Fig 4).

DISCUSSION

In this study, we demonstrated a lower CSF_{max} in patients with NPH compared with both age-matched and younger controls, which suggests a lower Windkessel effect and dampening of pulsations of the spinal CSF spaces. Physiologically, craniospinal CSF outflow compensates for systolic intracranial pressure peaks due to pulsatile arterial inflow.[24] Our results support new concepts that attribute the pathophysiology of NPH to abnormal dynamics of CSF and blood flow,[19–23] especially the concept of a reduced spinal CSF buffer function, represented by a low cervical CSF outflow.

The observed reduction of spinal CSF_{max} in patients with NPH could theoretically be due to a reduced arterial inflow to the brain during systole. However, our results of a reduced CSF_{max} in patients with NPH compared with HC-M and HC-Y remained significant, even when accounting for the potential effect of decreased arterial inflow in patients with NPH. The reduction of CSF_{max} in patients with NPH, therefore, exceeded the expected age-related changes. CSF_{max} could be a direct measure for the reduced compliance of spinal CSF spaces, ie, a reduced spinal buffer function or Windkessel effect, with the systolic peaks of intracranial pressure in patients with NPH not being compensated by CSF outflow. Our results complement the results of earlier studies on compliance of vessels and craniospinal CSF spaces.[30,31] These prior studies attributed the reduction of cervical CSF pulsations to an arterial loss of pulsatility[31] and assumed the reduced cervical CSF flow to be a consequence of a decreased arterial expansion due to pathologic changes of arteries and perivascular spaces.[30] Recent investigations were able to show that respiration

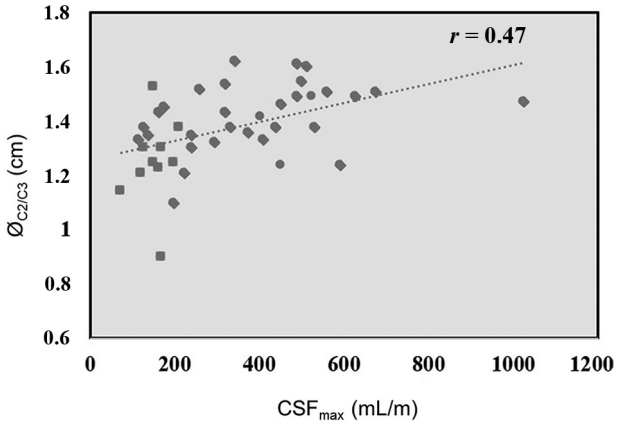

FIG 4. The relationship between spinal canal width and maximal CSF flow. Correlation analysis shows a positive correlation between CSF_{max} and $Ø_{C2/C3}$ ($r = 0.47$; $P < .05$).

and the cardiac cycle affect CSF flow at the cervical level.[32-34] Besides these influences, a general variation in the direction and magnitude of CSF flow is known to occur in both healthy individuals and patients with NPH,[35,36] with a redirectional[35] and mainly retrograde (ie, toward the ventricles) aqueductal flow[36] and a cranially directed CSF net flow at the craniocervical junction[36] in patients with NPH.

Another new concept that attributes the pathophysiology of NPH to abnormal CSF is that of a hyperdynamic CSF flow in the aqueduct.[19-23] Prior studies analyzed the relation between aqueductal CSF flow and the clinical response to the shunting procedure,[37,38] demonstrating that aqueductal CSF flow was not able to reliably predict clinical improvement after shunt implantation.[39,40] Aqueductal CSF flow seems to be strongly correlated with ventricular morphology,[41] showing higher aqueductal CSF oscillations in patients with NPH.[10-12] The lower craniospinal CSF_{max} in patients with NPH observed in our study might correspond to a higher CSF volume in the aqueduct, resulting in a higher oscillatory flow.[10-12] The higher CSF volume in the aqueduct[10-12] may be the consequence of a reduced Windkessel effect of the superior spinal CSF spaces, with CSF outflow from the brain being inefficient to buffer systolic intracranial pressure peaks.

Prior studies have investigated the age dependency of CSF flow values,[14,31,42-45] demonstrating age dependence of CSF flow parameter,[14,45] with significantly reduced CSF stroke volumes in the elderly.[31] However, Lokossou et al[44] suggested that aging mainly changes cerebral blood flow but preserves blood and CSF interactions, with an age-independent positive correlation between blood and CSF stroke volumes. Our results show a significantly lower CSF_{max} from the brain during systole in older participants compared with young healthy controls ($P < .05$), confirming prior results on age dependency of CSF flow. Additionally, our results show a lower CSF_{max} in patients with NPH compared with age-matched healthy controls, suggesting that the reduction of maximal craniospinal CSF flow in patients with NPH exceeds age-related changes. Our results complement the findings of Abdalla et al,[42] who differentiated patients with NPH from control subjects with mere age-related brain atrophy based on diverse CSF flow dynamics at the level of the aqueduct.

In our study, the diameter of the spinal canal at the level C2/C3 ($Ø_{C2/C3}$) was decreased in patients with NPH compared with both HC-M and HC-Y, and there was a positive correlation between the craniospinal CSF_{max} and $Ø_{C2/C3}$. The narrowing of the spinal canal may lead to a blocked craniospinal CSF flow with a reduced dampening of pulse pressure waves. This possibility could explain both the higher aqueductal CSF oscillations in patients with NPH[10–12] and the reduced craniospinal CSF_{max}. The spinal canal narrowing in patients with NPH may be secondary to degenerative changes that may involve hypertrophy and calcification of the ligaments, intervertebral discs, and osseous tissue.[46] Further studies are necessary to corroborate our findings and evaluate degenerative changes and spinal canal narrowing in patients with NPH.

There are several limitations to our study that need to be considered when interpreting the data. First, our sample sizes are limited. This was at least, in part, due to strict inclusion criteria for the NPH group, requiring at least 2 of the 3 symptoms of the Hakim triad and positive findings on a lumbar tap test without any indication for secondary hydrocephalus. We, nevertheless, were able to demonstrate a significantly reduced CSF_{max} in patients with NPH. Further studies with larger sample sizes will be needed to confirm our results. Second, diagnosing NPH remains challenging, and even with positive findings on a lumbar tap test, some risk of erroneously included patients remains. Finally, we assessed only the diameter of the spinal canal at the level of C2/C3. Further studies are needed to investigate additional spinal canal narrowing in lower segments.

CONCLUSIONS

We observed a reduction of maximal craniospinal CSF flow in patients with NPH compared with HC-M. This effect exceeded age-related changes of CSF flow and remained significant, even when accounting for differential arterial blood flow rates. A reduced compliance of spinal CSF spaces may play an important role in the etiopathogenesis of NPH. Systolic craniospinal CSF flow rates are an easily obtainable MR imaging–based measure that may support the diagnosis of NPH.

Disclosure forms provided by the authors are available with the full text and PDF of this article at www.ajnr.org.

REFERENCES

1. Adams RD, Fisher CM, Hakim S, et al. **Symptomatic occult hydrocephalus with "normal" cerebrospinal-fluid pressure: a treatable syndrome.** *N Engl J Med* 1965;273:117–26 CrossRef Medline
2. Graff-Radford NR, Godersky JC, Jones MP. **Variables predicting surgical outcome in symptomatic hydrocephalus in the elderly.** *Neurology* 1989;39:1601–04 CrossRef Medline
3. Marmarou A, Young HF, Aygok GA, et al. **Diagnosis and management of idiopathic normal-pressure hydrocephalus: a prospective study in 151 patients.** *J Neurosurg* 2005;102:987–97 CrossRef Medline
4. Kitagaki H, Mori E, Ishii K, et al. **CSF spaces in idiopathic normal pressure hydrocephalus: morphology and volumetry.** *AJNR Am J Neuroradiol* 1998;19:1277–84 Medline
5. Virhammar J, Laurell K, Cesarini KG, et al. **The callosal angle measured on MRI as a predictor of outcome in idiopathic normal-pressure hydrocephalus.** *J Neurosurg* 2014;120:178–84 CrossRef Medline

6. Ghosh S, Lippa C. **Diagnosis and prognosis in idiopathic normal pressure hydrocephalus.** *Am J Alzheimers Dis Other Demen* 2014;29:583–89 CrossRef Medline
7. Iddon JL, Pickard JD, Cross JJ, et al. **Specific patterns of cognitive impairment in patients with idiopathic normal pressure hydrocephalus and Alzheimer's disease: a pilot study.** *J Neurol Neurosurg Psychiatry* 1999;67:723–32 CrossRef Medline
8. Bradley WG, Whittemore AR, Kortman KE Jr, et al. **Marked cerebrospinal fluid void: indicator of successful shunt in patients with suspected normal-pressure hydrocephalus.** *Radiology* 1991;178:459–66 CrossRef Medline
9. Lee VS, Spritzer CE, Carroll BA, et al. **Flow quantification using fast cine phase-contrast MR imaging, conventional cine phase-contrast MR imaging, and Doppler sonography: in vitro and in vivo validation.** *AJR Am J Roentgenol* 1997;169:1125–31 CrossRef Medline
10. El Sankari S, Fichten A, Gondry-Jouet C, et al. **Correlation between tap test and CSF aqueductal stroke volume in idiopathic normal pressure hydrocephalus.** *Acta Neurochir Suppl* 2012;113:43–46 CrossRef Medline
11. El Sankari S, Gondry-Jouet C, Fichten A, et al. **Cerebrospinal fluid and blood flow in mild cognitive impairment and Alzheimer's disease: a differential diagnosis from idiopathic normal pressure hydrocephalus.** *Fluids Barriers CNS* 2011;8:12 CrossRef Medline
12. Shanks J, Markenroth Bloch K, Laurell K, et al. **Aqueductal CSF stroke volume is increased in patients with idiopathic normal pressure hydrocephalus and decreases after shunt surgery.** *AJNR Am J Neuroradiol* 2019;40:453–59 CrossRef Medline
13. Buijs PC, Krabbe-Hartkamp MJ, Bakker CJ, et al. **Effect of age on cerebral blood flow: measurement with ungated two-dimensional phase-contrast MR angiography in 250 adults.** *Radiology* 1998;209:667–74 CrossRef Medline
14. Schmid Daners M, Knobloch V, Soellinger M, et al. **Age-specific characteristics and coupling of cerebral arterial inflow and cerebrospinal fluid dynamics.** *PLoS One* 2012;7:e37502 CrossRef Medline
15. Bradley WG, Whittemore AR, Watanabe AS Jr, et al. **Association of deep white matter infarction with chronic communicating hydrocephalus: implications regarding the possible origin of normal-pressure hydrocephalus.** *AJNR Am J Neuroradiol* 1991;12:31–39 Medline
16. Ritter S, Dinh TT. **Progressive postnatal dilation of brain ventricles in spontaneously hypertensive rats.** *Brain Res* 1986;370:327–32 CrossRef Medline
17. Boon AJ, Tans JT, Delwel EJ, et al. **Dutch Normal-Pressure Hydrocephalus Study: the role of cerebrovascular disease.** *J Neurosurg* 1999;90:221–26 CrossRef Medline
18. Bradley WG. **Normal pressure hydrocephalus: new concepts on etiology and diagnosis.** *AJNR Am J Neuroradiol* 2000;21:1586–90 Medline
19. Kuriyama N, Tokuda T, Miyamoto J, et al. **Retrograde jugular flow associated with idiopathic normal pressure hydrocephalus.** *Ann Neurol* 2008;64:217–21 CrossRef Medline
20. Qvarlander S, Lundkvist B, Koskinen LO, et al. **Pulsatility in CSF dynamics: pathophysiology of idiopathic normal pressure hydrocephalus.** *J Neurol Neurosurg Psychiatry* 2013;84:735–41 CrossRef Medline
21. Bateman GA. **Vascular compliance in normal pressure hydrocephalus.** *AJNR Am J Neuroradiol* 2000;21:1574–85 Medline
22. Owler BK, Pickard JD. **Normal pressure hydrocephalus and cerebral blood flow: a review.** *Acta Neurol Scand* 2001;104:325–42 CrossRef Medline
23. Silverberg GD. **Normal pressure hydrocephalus (NPH): ischaemia, CSF stagnation or both.** *Brain* 2004;127:947–48 CrossRef Medline
24. Shprecher D, Schwalb J, Kurlan R. **Normal pressure hydrocephalus: diagnosis and treatment.** *Curr Neurol Neurosci Rep* 2008;8:371–76 CrossRef Medline
25. Nakajima M, Yamada S, Miyajima M, et al; research committee of idiopathic normal pressure hydrocephalus. ***Guidelines for Management of Idiopathic Normal Pressure Hydrocephalus* (Third Edition): endorsed by the Japanese Society of Normal Pressure Hydrocephalus.** *Neurol Med Chir (Tokyo)* 2021;61:63–97 CrossRef Medline
26. Williams MA, Relkin NR. **Diagnosis and management of idiopathic normal-pressure hydrocephalus.** *Neurol Clin Pract* 2013;3:375–85 CrossRef Medline
27. Tain RW, Ertl-Wagner B, Alperin N. **Influence of the compliance of the neck arteries and veins on the measurement of intracranial volume change by phase-contrast MRI.** *J Magn Reson Imaging* 2009;30:878–83 CrossRef Medline
28. Alperin N, Mazda M, Lichtor T, et al. **From cerebrospinal fluid pulsation to noninvasive intracranial compliance and pressure measured by MRI flow studies.** *Current Medical Imaging Reviews* 2006;2:117–29 CrossRef
29. Alperin N, Lee SH. **PUBS: Pulsatility-based segmentation of lumens conducting non-steady flow.** *Magn Reson Med* 2003;49:934–44 CrossRef Medline
30. Greitz D, Hannerz J, Rahn T, et al. **MR imaging of cerebrospinal fluid dynamics in health and disease: on the vascular pathogenesis of communicating hydrocephalus and benign intracranial hypertension.** *Acta Radiology* 1994;35:204–211 Medline
31. Stoquart-ElSankari S, Balédent O, Gondry-Jouet C, et al. **Aging effects on cerebral blood and cerebrospinal fluid flows.** *J Cereb Blood Flow Metab* 2007;27:1563–72 CrossRef Medline
32. Daouk J, Bouzerar R, Baledent O. **Heart rate and respiration influence on macroscopic blood and CSF flows.** *Acta Radiol* 2017;58:977–82 CrossRef Medline
33. Dreha-Kulaczewski S, Konopka M, Joseph AA, et al. **Respiration and the watershed of spinal CSF flow in humans.** *Sci Rep* 2018;8:5594 CrossRef Medline
34. Vinje V, Ringstad G, Lindstrøm EK, et al. **Respiratory influence on cerebrospinal fluid flow - a computational study based on long-term intracranial pressure measurements.** *Sci Rep* 2019;9:9732 CrossRef Medline
35. Eide PK, Valnes LM, Lindstrom EK, et al. **Direction and magnitude of cerebrospinal fluid flow vary substantially across central nervous system diseases.** *Fluids Barriers CNS* 2021;18:16 CrossRef Medline
36. Lindstrom EK, Ringstad G, Mardal KA, et al. **Cerebrospinal fluid volumetric net flow rate and direction in idiopathic normal pressure hydrocephalus.** *Neuroimage Clin* 2018;20:731–41 CrossRef Medline
37. Bradley WG, Scalzo D, Queralt J Jr, et al. **Normal-pressure hydrocephalus: evaluation with cerebrospinal fluid flow measurements at MR imaging.** *Radiology* 1996;198:523–29 CrossRef Medline
38. Sharma AK, Gaikwad S, Gupta V, et al. **Measurement of peak CSF flow velocity at cerebral aqueduct, before and after lumbar CSF drainage, by use of phase-contrast MRI: utility in the management of idiopathic normal pressure hydrocephalus.** *Clin Neurol Neurosurg* 2008;110:363–68 CrossRef Medline
39. Dixon GR, Friedman JA, Luetmer PH, et al. **Use of cerebrospinal fluid flow rates measured by phase-contrast MR to predict outcome of ventriculoperitoneal shunting for idiopathic normal-pressure hydrocephalus.** *Mayo Clin Proc* 2002;77:509–14 CrossRef Medline
40. Blitz AM, Shin J, Balédent O, et al. **Does phase-contrast imaging through the cerebral aqueduct predict the outcome of lumbar CSF drainage or shunt surgery in patients with suspected adult hydrocephalus?** *AJNR Am J Neuroradiol* 2018;39:2224–30 CrossRef Medline
41. Chiang WW, Takoudis CG, Lee SH, et al. **Relationship between ventricular morphology and aqueductal cerebrospinal fluid flow in healthy and communicating hydrocephalus.** *Invest Radiol* 2009;44:192–99 CrossRef Medline
42. Abdalla RN, Ghani Zghair MA. **The role of magnetic resonance imaging cerebrospinal fluid flowmetry in differentiation between normal flow hydrocephalus and involutional brain atrophy.** *J Pak Med Assoc* 2019;69:S78–82 Medline

43. Di Palma C, Goulay R, Chagnot S, et al. **Cerebrospinal fluid flow increases from newborn to adult stages.** *Dev Neurobiol* 2018;78:851–58 CrossRef Medline
44. Lokossou A, Metanbou S, Gondry-Jouet C, et al. **Extracranial versus intracranial hydro-hemodynamics during aging: a PC-MRI pilot cross-sectional study.** *Fluids Barriers CNS* 2020;17:1 CrossRef Medline
45. Sartoretti T, Wyss M, Sartoretti E, et al. **Sex and age dependencies of aqueductal cerebrospinal fluid dynamics parameters in healthy subjects.** *Front Aging Neurosci* 2019;11:19 CrossRef Medline
46. Moghaddamjou A, Badhiwala JH, Fehlings MG. **Degenerative cervical myelopathy: changing frontiers.** *World Neurosurg* 2020;135:377–78 CrossRef Medline